



Single-shot carrier-envelope-phase detection using tunneling ionization in ambient air

**BIN KIM,^{1,2} JEONG-UK SHIN,^{1,2} WOSIK CHO,² YANG HWAN KIM,²
KYUNG HOON YEOM,^{1,2} AND KYUNG TAEC KIM^{1,2,*} **

¹*Department of Physics and Photon Science, Gwangju Institute of Science and Technology, Gwangju 61005, Republic of Korea*

²*Center for Relativistic Laser Science, Institute for Basic Science, Gwangju 61005, Republic of Korea*
**kyungtaec@gist.ac.kr*

Abstract: The carrier-envelope phase (CEP) of a laser pulse plays a crucial role in laser-matter interactions. The inherent shot-to-shot instability of the CEP necessitates single-shot detection, which is not only vital for stabilizing the CEP but also for observing ultrafast phenomena that conventional averaging techniques cannot resolve. In this study, we demonstrate a novel approach utilizing strong-field ionization in ambient air for single-shot CEP measurement. Our method is applicable without the need for an imaging device, providing a practical and precise solution for high-repetition-rate CEP measurement.

© 2024 Optica Publishing Group under the terms of the [Optica Open Access Publishing Agreement](#)

1. Introduction

The carrier-envelope phase (CEP) of an ultrashort laser pulse is an important parameter that describes the phase difference between the carrier wave and the envelope of the pulse. It is crucial in strong-field physics and attosecond science, as it plays a critical role in determining the outcome of laser-matter interactions. Specifically, the CEP of the laser pulse affects strong-field ionization and the electron trajectory after ionization, leading to differences in various phenomena such as above-threshold ionization [1], high harmonic generation [2], and frustrated tunneling ionization [3]. Therefore, measuring the CEP is essential for understanding and controlling laser-driven phenomena in atoms, molecules, and solids.

Over the past two decades, several techniques have been developed for the CEP measurement. One commonly used method is the f-to-2f interferometer [4,5], which determines the CEP by measuring the interference between the second harmonic of the fundamental pulse and the same frequency component inherited from the fundamental pulse. The f-to-2f technique has become a widely used method for producing a feedback signal to stabilize the CEP, utilizing the interference between a broadband laser pulse and its second harmonic pulse. This technique provides information on the variation of the CEP, which corresponds to the relative changes in CEP between consecutive laser shots.

The absolute CEP of individual laser shots could be measured by utilizing above-threshold ionization (ATI) spectra measured using a stereo ATI spectrometer [1,6,7]. These techniques rely on the observation that the probability of electrons being detected in the two opposite directions of the laser polarization depends on the laser pulse's CEP. The stereo ATI spectrometer is a powerful tool for measuring the absolute value of the CEP in a single-shot.

To overcome the complexity of the ATI-based measurements in vacuum, other experimental approaches were proposed that operate in ambient air [8–14]. One of the recent methods involves the use of nanostructures [8–11]. When a laser pulse hits a nanostructure, the plasmonic effect enhances the laser field. By utilizing the CEP dependence of the photoemission current induced by the enhanced field, the CEP of the enhanced field could be measured. Another method recently demonstrated involves utilizing pulses of circular polarization to ionize the air and detecting the generated currents in different directions [13].

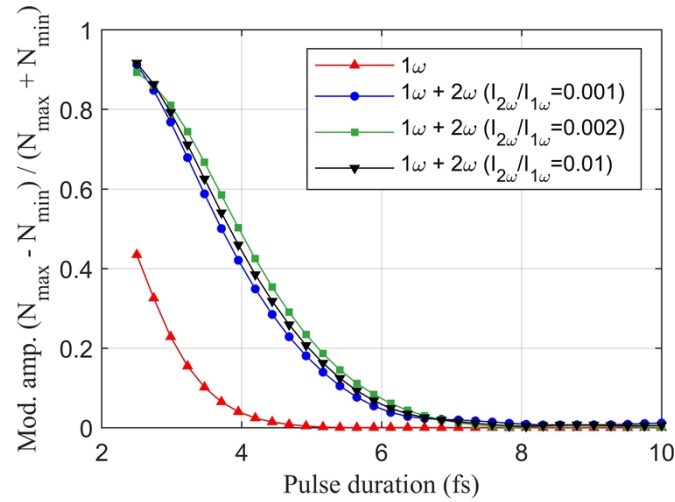


Fig. 1. Normalized amplitude of ionization yield modulations. The ionization yields are obtained by solving the time-dependent Schrödinger equation (1D) for different CEPs. Then, the normalized amplitude of the ionization yield modulation $[(N_{max} - N_{min})/(N_{max} + N_{min})]$ is obtained using the maximum (N_{max}) and minimum (N_{min}) values. It is assumed that the laser field has a Gaussian envelope $A(t)$ at the center wavelength of $\lambda_1 = 800$ nm. For the two color cases ($\lambda_1 = 800$ nm and $\lambda_2 = 400$ nm), the phase of the second harmonic field is set to be twice of the phase of the fundamental field [i.e. $E_{1\omega}(t) = A_{1\omega}(t) \cos(\omega_1 t + \phi_{CEP})$ and $E_{2\omega}(t) = A_{2\omega}(t) \cos(2\omega_1 t + 2\phi_{CEP})$, where ω_1 is the carrier frequency of the fundamental pulse, t the time, ϕ_{CEP} the CEP of the fundamental pulse]. The FWHMs for fundamental pulse and second harmonic pulse are 5fs and 20fs, respectively. The intensity of the fundamental pulse is fixed to be 10^{13} W/cm², and the intensity ratios are shown in the legend.

We present a new approach for a single-shot CEP measurement using strong-field ionization in ambient air. Ionization yields produced by two-color laser fields are obtained at different relative phases. The ionization yields provide information on the absolute CEP value of the laser pulse. Since the method can be combined with a pulse characterization technique called tunneling ionization with a perturbation for the time-domain observation of an electric field (TIPTOE) method [14], complete information on the incident laser pulse can be obtained. Also, it can be implemented using a relatively simple experiment setup in ambient air without changing the polarization state of the incident laser pulse. Therefore, our approach will be used as an important tool for CEP measurements.

2. Basic principle of CEP measurement using ionization

The temporal waveform of a laser field varies depending on the CEP. This effect becomes clear when the pulse is short. The variation of the CEP causes a significant impact on strong field ionization and the electron trajectory after the ionization. The ATI spectra show a clear difference even for few-cycle driving laser pulses. Thus, the CEP of the laser pulse can be determined by measuring the photoelectron spectra using a photoelectron spectrometer [4].

The amount of ionization is also dependent on the CEP of the laser pulse, which can be easily measured in ambient air [15]. We calculated the variation of the ionization yield $N(\phi_{CEP})$ for different CEPs ϕ_{CEP} by solving the time-dependent Schrödinger equation. A sinusoidal modulation of the ionization yields was observed as the CEP varies. The normalized amplitude of the modulation $[(N_{max} - N_{min})/(N_{max} + N_{min})]$ could be obtained using the maximum (N_{max}) and

the minimum (N_{min}) values of the ionization yield modulation, as shown in Fig. 1. We calculated the normalized amplitude of the ionization yield modulation for different pulse durations. The normalized amplitude of the modulation increases as the duration of the laser pulse decreases as shown in Fig. 1.

The ionization yield is also highly sensitive to other laser parameters, such as power, polarization, divergence, and dispersion conditions. For example, a power fluctuation of 1% can change the ionization yield in air by approximately 6% [14]. Therefore, to determine the CEP of the laser pulse from the ionization yield, the amplitude of the ionization yield modulation should be sufficiently large. However, the calculation results shown in Fig. 1 suggest that the pulse duration needs to be nearly as short as a single-cycle pulse (2-3 fs duration at a wavelength of 800 nm) to observe significant variation in the ionization yield for different CEPs, which imposes stringent requirements on many applications.

We use a second harmonic field of the fundamental laser field to mitigate the duration requirement. By mixing the second harmonic field with the fundamental laser field, the duration of the laser pulse effectively reduces, and the modulation amplitude is enhanced, as shown in Fig. 1. We obtained the largest modulation amplitude when the intensity ratio between the fundamental ($I_{1\omega}$) and second harmonic ($I_{2\omega}$) pulses is $I_{2\omega}/I_{1\omega} \sim 0.002$. For a two-cycle laser pulse (5.2 fs at the wavelength of 800 nm), the modulation amplitude is 0.2, significantly higher than 0.002, the value obtained with a single-color laser pulse, as shown in Fig. 1. Consequently, the CEP of the laser pulse can be measured using a two-color laser field under relaxed conditions.

3. Experimental setup

For the experimental demonstration of the CEP measurement, we used a CEP-stabilized Ti:sapphire laser (Femtopower X CEP4, Femtolaser). The output pulse of the laser system has a center wavelength of 800 nm and a duration of 30 fs. It was compressed down to 5 fs using a stretched-hollow-core fiber and an array of chirped mirrors [16]. The CEP of the laser pulse was stabilized using the feed-forward scheme [17]. For comparison, an f-2f interferometer was installed. The laser beam partially reflected on the glass wedge was used for the f-2f interferometer as shown in Fig. 2(a). The CEP was controlled by changing the thickness of the fused silica wedge.

In order to measure an ionization yield, we used a TIPTOE setup that is used for the temporal characterization of the laser field [13]. An input laser beam is divided into two replica beams using an annular mirror and an inner mirror as shown in Fig. 2(a). A main pulse (reflected by the annular mirror) is responsible for inducing ionization. A weak pulse, which on its own cannot produce ionization, can modulate the ionization yield when it is superposed on the main pulse. The temporal profile of the weak laser field is obtained by the modulation of the ionization yield in air molecules (mostly O_2). Here, we applied a bias voltage of ~ 1 kV to the electrodes to prevent the recombination of ionized electrons with ions [18]. This configuration allows for a large separation between the electrodes (2 mm), which is significantly greater than the size of the focused beam. The TIPTOE setup is insensitive to alignment changes of the laser beam. However, this configuration is also insensitive to the directionality of the ionization, meaning that we can only measure the amount of ionization [13,15].

The TIPTOE setup is designed for the temporal characterization of a laser pulse, but it is also useful for CEP measurement. We placed a Type-1 BBO crystal in the beam path to create the second harmonic field, as shown in Fig. 2(a). Since the fundamental pulse is significantly stronger than the second harmonic and their polarizations are orthogonal, we used a wire-grid polarizer to control the relative intensity and polarization. After the wire-grid polarizer, the fundamental beam is significantly attenuated, and both beams have the same polarization. The peak intensity of the fundamental pulse was approximately 7×10^{12} W/cm². The intensity ratio between the second harmonic and the fundamental was $I_{2\omega}/I_{1\omega} \cong 0.01$.

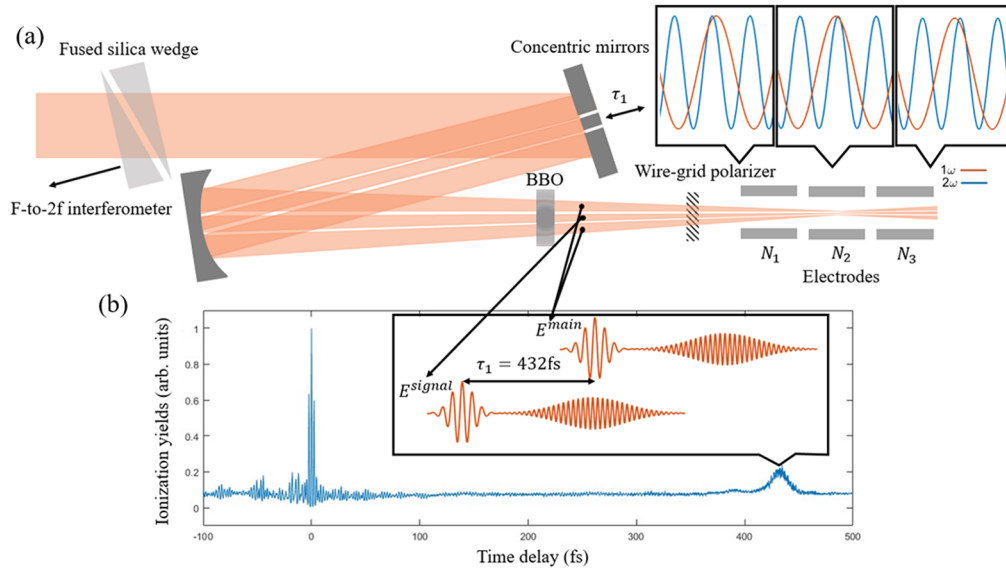


Fig. 2. A schematic diagram of the experimental setup. (a) TIPTOE setup. The reflected beam on the glass wedge is used for the f-2f interferometer. The incident beam is split using the annular mirror and the inner mirror. The annular mirror has a hole (2.6 mm), and the diameter of the inner mirror is 2 mm. A BBO crystal (0.2 mm thickness, Type-1) is used to produce a second harmonic field. The two beams are focused with a focusing with an f-number of 125. The wire-grid polarizer is used to adjust the intensity ratio between the fundamental and second harmonic fields. The ionization yields (N_1 , N_2 , and N_3) are measured using three electrodes separated by 30 mm. The fundamental of the main pulse overlaps with the second harmonic of the signal pulse with different phases at three electrodes due to the Gouy phase and air dispersion. (b) Ionization yield modulation obtained with two-color laser fields. The inset shows the main and signal pulses with a time delay of 432 fs.

Since the second harmonic pulse is delayed with respect to the fundamental pulse after the second harmonic generation, they do not overlap in time. There are four pulses: the main pulse has the fundamental and second harmonic fields, and the weak signal pulse also has the fundamental and second harmonic fields, as shown in the inset of Fig. 2(b). We adjust the time delay between the main and signal pulses so that the fundamental of the main pulse overlaps with the second harmonic of the signal pulse. To find the temporal overlap of these pulses, we measured the ionization yield as a function of the delay between the main and signal pulses.

The TIPTOE trace shows a few-cycle pulse near a delay of zero that corresponds to the fundamental 5fs pulse. At a delay of 432 fs, we observed an increase in the ionization yield due to the overlap of the fundamental pulse of the main pulse and the second harmonic of the signal pulse as illustrated in the inset in Fig. 2(b). In this case, the second harmonic pulse of the main pulse ($E_{2\omega}^{main}$) and the fundamental pulse of the signal pulse ($E_{1\omega}^{signal}$) do not contribute to the ionization yield because they are too weak. The ionization yield is produced by the combination of the two fields ($E_{1\omega}^{main} + E_{2\omega}^{signal}$) as shown in the inset in Fig. 2(b). Using this experimental setup, we could control the CEP and the relative phase of the two-color laser field. It should be noted that the ionization probability is very low ($<10^{-8}$) [15]. We did not observe any noticeable changes in the spectrum of the laser beam after the focus.

For the two-color laser field, the ionization yield is dependent on both the CEP and the relative phase. We have calculated the ionization yield for the two-color laser field using the two laser fields, $A_{1\omega}(t) \cos(\omega_1 + \phi_{1\omega}) + A_{2\omega}(t) \cos(2\omega_1 + 2\phi_{1\omega} + \phi_{2\omega})$, as shown in Fig. 3(a). Since the

second harmonic is generated using the fundamental pulse, the phase of the second harmonic is dependent on the CEP of the fundamental pulse $\phi_{1\omega}$ with an additional phase ϕ_{20} . The ionization yield varies periodically depending on the CEP $\phi_{1\omega}$ and the additional phase ϕ_{20} , as shown in Fig. 3(a).

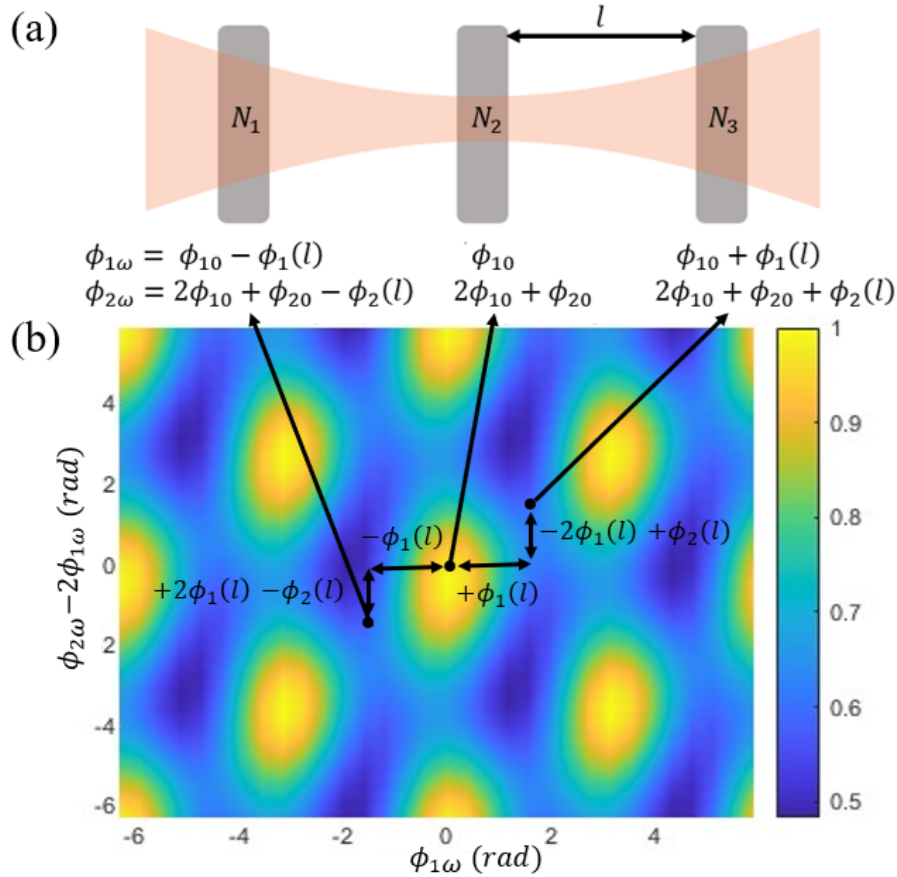


Fig. 3. (a) The phase difference between the fundamental and second harmonic pulses for three copper plates, N_1 , N_2 , and N_3 , where the $\phi_1(l)$ and $\phi_2(l)$ were calculated as $0.015\pi/\text{mm}$ and $0.1\pi/\text{mm}$, respectively, for an 8-mm beam. (b) The ionization yields as a function of ϕ_{10} and ϕ_{20} at N_2 . For N_1 and N_3 , it can be described by its phase shift. The black dots correspond to the ionization yields at N_1 , N_2 , and N_3 respectively. The positions of the black dots vary depending on $\phi_1(l)$ and $\phi_2(l)$.

In order to determine the CEP of the laser field with a single laser shot, we measure the ionization yield at three different positions near the focus, as shown in Fig. 3(b). These measurements allow us to measure the ionization yield with three different CEPs and relative phases with a single laser shot.

We analyze the ionization yields (N_1 , N_2 , and N_3) measured using three electrodes at different positions, as shown in Fig. 3(b). Here, ϕ_{10} represents the CEP of the fundamental pulse in the middle electrode, and ϕ_{20} represents the additional phase caused by a second harmonic generation process and propagation from the second harmonic crystal to the middle electrode. The first and third electrodes are equally separated from the middle electrode. Assuming the middle electrode is located at the focus, the phase differences caused by the Gouy phase shift and air dispersion

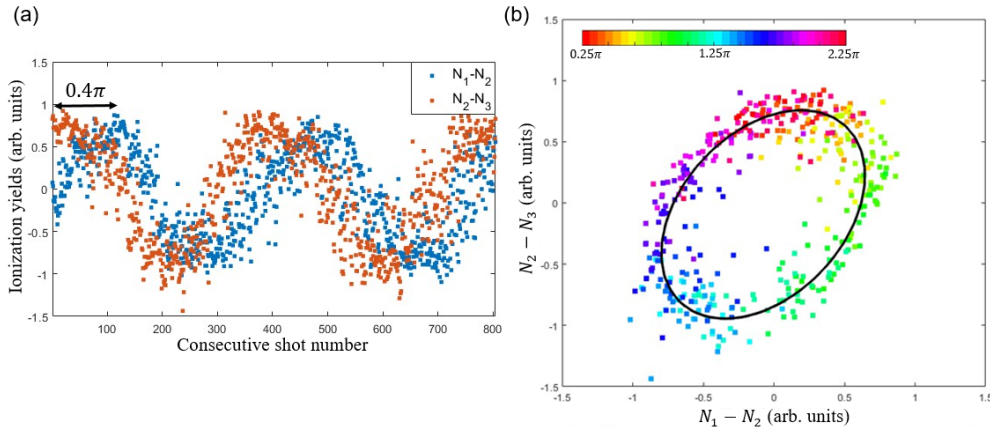


Fig. 4. (a) The ionization difference between the two copper plates was plotted as a function of shot number. Comparison with Fig. 4 reveals that shot numbers 1-12 correspond to the point of absolute CEP at $\pi/4$. (b) The CEP map with an elliptical fit was obtained from 1-372 shot number of (a), with each color corresponding to a specific CEP distribution of 2π range. The offset value was excluded in order to place the origin of the ellipse at the center.

are dependent on the distance between the electrodes, imposing additional phases [$\pm\phi_1(l)$ and $\phi_2(l)$] for the fundamental and second harmonic pulses.

The goal of this experiment is to create a parametric plot of a circular shaped object using the ionization levels in two channels, and to detect the absolute CEP value of N_2 in a single-shot. To minimize noise caused by intensity fluctuations, $N_1 - N_2$ and $N_2 - N_3$ were used for x-y axes, and a circular plot can be obtained when there is a phase difference of $\pi/2$ between the two axes.

The amount of the ionization yield varies depending on ϕ_{10} and ϕ_{20} . As the CEP (ϕ_{10}) of the fundamental pulse varies, the ionization amplitude modulates. This modulation is maximized when ϕ_{20} is 0 or $\pm\pi$. Therefore, we can find this condition by the ionization yield modulation of N_2 . Then, we have to find the distance l that determines $\phi_1(l)$ and $\phi_2(l)$. These two phases are related. When $\phi_1(l) = \pi/2$ and $\phi_2(l) = \pi$, we obtained the phase difference of approximately $\pi/2$ for the two axes. We can determine the optimal separation distance l by the phase difference of the two modulations ($N_1 - N_2$) and ($N_2 - N_3$).

4. Measurement results

We performed the single-shot CEP measurement using the Ti:sapphire laser that produces 30 fs pulses. The laser pulse is compressed using a stretched hollow core fiber and chirped mirrors down to 5 fs. The ionization yield differences obtained for different CEPs are measured as shown in Fig. 4(a). The ionization yields are obtained for 12 shots at the same CEP, and we changed the CEP slightly. As we change the CEP value, we observe sinusoidal modulations as expected. The ionization yield differences $N_1 - N_2$ and $N_2 - N_3$ have a phase difference of 0.4π . We can produce a circular plot using these two ionization yield differences for x and y axes, as shown in Fig. 4(b). The polar angle of this plot, which can be obtained by $\tan^{-1}[(N_2 - N_3)/(N_1 - N_2)]$ corresponds to the CEP of the fundamental laser field. The CEP measured through the polar angle in Fig. 4 and the CEP calculated through the thickness of fused silica wedges are compared in Fig. 5.

There are several sources of uncertainty in the CEP measurement, including fluctuations in intensity, dispersion conditions, and wavefront variations. These variations eventually affect the beam intensity, changing the ionization yields. In order to suppress these measurement errors, we introduced the ionization yield differences which form a circular plot. From this measurement, we could determine the CEP with a single laser shot.

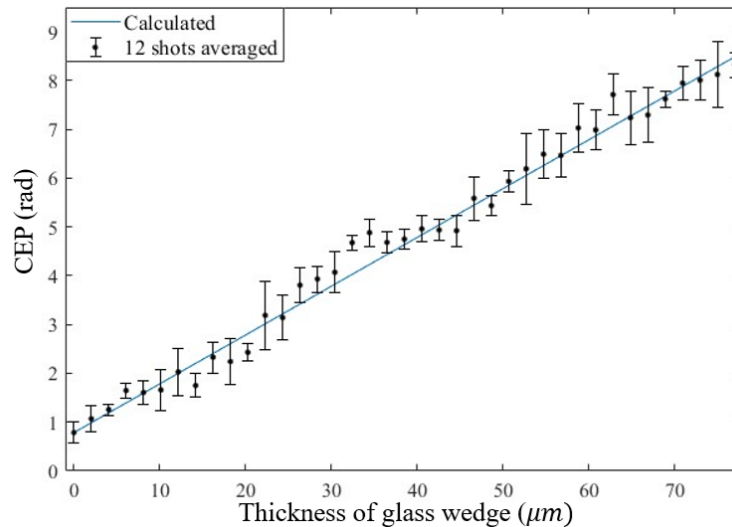


Fig. 5. Absolute CEPs obtained from the polar angle of the parametric plot. The CEP was controlled by a glass wedge. The CEP values of 12 laser shots were measured at a fixed wedge position. The average value of the 12 CEP measurements is shown with black dots and their standard deviation is represented with error bars. The expected CEP values calculated using the thickness of the fused silica wedges are shown with a blue line. The offset of the blue line is adjusted.

5. Conclusion

In this study, we successfully demonstrated the single-shot detection of the carrier-envelope phase (CEP) of few-cycle laser pulses using tunneling ionization in ambient air. We analyzed the ionization yields generated by two-color laser fields. It is shown that the ionization yields are modulated as the CEP of the fundamental pulse or the relative phase between the two pulses varies. We measured the ionization yields at three different positions, which allowed us to measure the ionization yields at different CEPs and relative phases simultaneously. Consequently, we could determine the CEP of the laser field with a single laser shot. We observed excellent agreement between the variations in the CEP induced by the thickness of the wedge glass and the period of ionization modulation, validating our theoretical predictions.

The single-shot measurement of CEP is crucial for precisely characterizing the waveform of few-cycle pulses and investigating the properties of the attosecond pulses they generate. It enables the determination of optical pulse characteristics at the attosecond scale, providing essential information for designing and manipulating laser pulses in interactions with molecules and solid materials.

The key advantages of our measurement method lie in its ‘single-shot’ capability and its operation in ‘ambient air’. The single-shot nature allows for effective response to rapidly changing fluctuations, as each pulse is individually tagged, unlike conventional time-averaging methods. Moreover, compared to existing single-shot techniques such as stereo above-threshold ionization (ATI), our method offers a simplified experimental setup without the need for a vacuum chamber. Also, the ionization measurement can be performed without using a slow device like a CCD camera. Thus, the CEP signal obtained from the ionization measurement can be directly converted with a very high repetition rate. Consequently, our method can provide real-time information about the pulses used in experiments, accurately capturing their characteristics without introducing changes in polarization or chirp.

Acknowledgments. This work was supported by the Institute for Basic Science grant (IBS-R012-D1) and the National Research Foundation of Korea (NRF), grant funded by the Korea government (MIST) (No. 2022R1A2C3006025) and (No. RS-2023-00218180).

Disclosures. The authors declare no potential conflicts of interest.

Data availability. Data underlying the results presented in this paper are not publicly available at this time but may be obtained from the authors upon reasonable request.

References

1. T. Wittmann, B. Horvath, W. Helml, *et al.*, “Single-shot carrier–envelope phase measurement of few-cycle laser pulses,” *Nat. Phys.* **5**(5), 357–362 (2009).
2. S. Ghimire and D. A. Reis, “High-harmonic generation from solids,” *Nat. Phys.* **15**(1), 10–16 (2019).
3. H. Yun, J. H. Mun, S. I. Hwang, *et al.*, “Coherent extreme-ultraviolet emission generated through frustrated tunnelling ionization,” *Nat. Photonics* **12**(10), 620–624 (2018).
4. D. J. Jones, S. A. Diddams, J. K. Ranka, *et al.*, “Carrier-envelope phase control of femtosecond mode-locked lasers and direct optical frequency synthesis,” *Science* **288**(5466), 635–639 (2000).
5. R. Holzwarth, Th. Udem, T. W. Hänsch, *et al.*, “Optical Frequency Synthesizer for Precision Spectroscopy,” *Phys. Rev. Lett.* **85**(11), 2264–2267 (2000).
6. G. G. Paulus, F. Grasbon, H. Walther, *et al.*, “Absolute-phase phenomena in photoionization with few-cycle laser pulses,” *Nature* **414**(6860), 182–184 (2001).
7. P. Dietrich, F. Krausz, and P. B. Corkum, “Determining the absolute carrier phase of a few-cycle laser pulse,” *Opt. Lett.* **25**(1), 16–18 (2000).
8. M. Krüger, M. Schenk, and P. Hommelhoff, “Attosecond control of electrons emitted from a nanoscale metal tip,” *Nature* **475**(7354), 78–81 (2011).
9. T. Rybka, M. Ludwig, M. F. Schmalz, *et al.*, “Sub-cycle optical phase control of nanotunnelling in the single-electron regime,” *Nat. Photonics* **10**(10), 667–670 (2016).
10. B. Piglosiewicz, S. Schmidt, D. J. Park, *et al.*, “Carrier-envelope phase effects on the strong-field photoemission of electrons from metallic nanostructures,” *Nat. Photonics* **8**(1), 37–42 (2014).
11. Y. Yang, M. Turchetti, P. Vasireddy, *et al.*, “Light phase detection with on-chip petahertz electronic networks,” *Nat. Commun.* **11**(1), 3407 (2020).
12. Y. Liu, J. E. Beetar, J. Nesper, *et al.*, “Single-shot measurement of few-cycle optical waveforms on a chip,” *Nat. Photonics* **16**(2), 109–112 (2022).
13. M. Kubullek, Z. Wang, K. Von Der Brelje, *et al.*, “Single-shot carrier–envelope-phase measurement in ambient air,” *Optica* **7**(1), 35 (2020).
14. S. B. Park, K. Kim, W. Cho, *et al.*, “Direct sampling of a light wave in air,” *Optica* **5**(4), 402–408 (2018).
15. W. Cho, Y. H. Kim, I. A. Ivanov, *et al.*, “Ionization yield measurement using metal electrodes with a static electric field in ambient air,” *J. Phys. B: At. Mol. Opt. Phys.* **53**(17), 174003 (2020).
16. S. I. Hwang, S. B. Park, J. Mun, *et al.*, “Generation of a single-cycle pulse using a two-stage compressor and its temporal characterization using a tunnelling ionization method,” *Sci. Rep.* **9**(1), 1613 (2019).
17. S. Koke, C. Grebing, H. Frei, *et al.*, “Direct frequency comb synthesis with arbitrary offset and shot-noise-limited phase noise,” *Nat. Photonics* **4**(7), 462–465 (2010).
18. W. Cho, S. I. Hwang, C. H. Nam, *et al.*, “Temporal characterization of femtosecond laser pulses using tunneling ionization in the UV, visible, and mid-IR ranges,” *Sci. Rep.* **9**(1), 16067 (2019).